

Electronic Supplementary Information (ESI)

TiO₂ Nanodisk Designed for Li-ion Batteries: A Novel Strategy of Obtaining Ultrathin and High Surface Area Anode Material at Ice Interface

Gonu Kim[†], Changshin Jo[†], Wooyul Kim, Jinyoung Chun, Songhun Yoon, Jinwoo Lee* and Wonyong Choi*

1. Experimental Details
 - 1) Synthesis of TiO₂ nanodisk powder
 - 2) Synthesis of colloidal 2-D TiO₂-ice and colloidal TiO₂ nanoparticle
 - 3) Material Characterization
 - 4) Electrochemical Characterization
2. Text S1, Fig. S1~6, Table S1~S2
3. References

1. Experimental Details

1) Synthesis of TiO₂ nanodisk powder: 100 mL of deionized (DI) water was frozen in a refrigerator for more than 12h. Ultrapure (18 MΩcm) deionized water was prepared by a Barnstead purification system and the temperature of a refrigerator was -17 °C. The prepared ice was cracked into small pieces by an ice-breaker and obtained pieces of ice were added to 200 mL of normal-hexane (n-hexane) (Samchun, Korea) solvent which contains 0.5 mL of titanium (IV) isopropoxide (TTIP, Junsei). After slight stirring for a second, the n-hexane solvent was poured out and 100 mL of ethanol (J. T. Baker) was added into the ice pieces. White TiO₂ precipitate was obtained by filtering the above prepared solution and washed with 1L of DI water. The resulting TiO₂ nanodisk powder was dried in an oven at 80 °C for 12 h.

2) Synthesis of colloidal 2-D TiO₂-ice and colloidal TiO₂ nanoparticle: Synthetic procedure for colloidal 2-D TiO₂-ice was similar to that for TiO₂ nanodisk powder. After synthesizing 2-D TiO₂-ice on the surface of ice by the above process, n-hexane solvent was poured out and we added 100 mL of ethanol which containing 1mL of hydrochloric acid (HCl, Sigma-Aldrich, 37%). After adding the ethanol solution into remaining pieces of ice, this solution was evaporated at 50°C. White color of the solution became transparent as the solvent evaporated. The transparent colloidal 2-D TiO₂-ice solution was collected before the solvent was completely evaporated. The synthesis of colloidal TiO₂ nanoparticle followed the literature method.^[1] 5 mL of 2-propanol (Junsei) was added to 30 mL of TTIP (Junsei) and this mixture was added to 180 mL of DI water. 2 mL of HCl (Sigma-Aldrich, 37%) was added to above solution and then the solution was heated at 80 °C for 8 h. Final powder product was obtained by evaporating the solvent under low pressure using a rotatory evaporator.

3) Material Characterization: The phase identification of TiO₂ nanodisk was carried out by powder X-ray diffraction (XRD) using Cu K α radiation (Mac Science Co. M18XHF). The N₂ physisorption analysis for BET surface area and pore size distribution was conducted using Micromeritics Tristar II. For AFM analysis, TiO₂ samples were diluted with 50% (v/v) water/ethanol solution and then dispersed by strong sonication process. Samples for AFM measurements were prepared by loading a drop of diluted solution of the TiO₂ nanodisk powder or Degussa P25 on the mica substrate. Atomic force microscopy (AFM) measurement was carried out in tapping mode using a scanning probe microscope (SPM, Veeco Dimension 3100 + Nanoscope V). The morphologies of TiO₂ samples were analyzed by high-resolution transmission electron microscopy (HR-TEM, JEOL JEM-2200 FS) and field-emission scanning electron microscopy (FE-SEM, JEOL JSM-7401F). For the analysis of AFM, HR-TEM, FE-SEM, TiO₂ nanodisk powder was dried in an oven at 80 °C and Degussa P25 was used as received. Absorption measurements were carried out with a UV/visible spectrophotometer (Agilent 8453).

4) Electrochemical Characterization: For the preparation of electrodes, the TiO₂ nanodisk or Degussa P25 powder was separately mixed with conducting carbon (Super P) and a polyvinylidene difluoride (PVDF) binder (8:1:1 in weight ratio) in *N*-methyl-2-pyrrolidone (NMP). The slurry was coated on a Cu foil. After drying at 80 °C in vacuum oven more than 1 day, the electrode was pressed and cut. The half-cell test was conducted with a coin-type two electrode cell (CR2032). The lithium foil was used as both counter and reference electrodes. The electrolyte was 1.0 M LiPF₆ in ethylene carbonate/dimethyl carbonate (EC/DMC, 1:1 volume ratio, Panaxetec Co., Korea). The galvanostatic charge/discharge test was conducted in the potential range of 3.0 to 1.0 V (vs. Li/Li⁺) using a WBCS-3000 battery cycler (Xeno Co.). The cyclic voltammetry test was performed in the 3.0 to 1.0 V (vs. Li/Li⁺) range using a

Reference 600 potentiostat (Gamry Instruments, USA). The electrochemical impedance spectroscopy (EIS) analysis was conducted at $E \approx 1.7$ V after 5 charge/discharge cycles. The frequency range was 10^5 to 0.01 Hz under ac stimulus with 5 mV amplitude using Reference 600 potentiostat (Gamry Instruments, USA).

Text S1

The bandgap shift, ΔE_g , of a two-dimensional crystallites is given by^[2]

$$\Delta E_g = \frac{h^2}{4\mu_{xy}L_{xy}^2} + \frac{h^2}{8\mu_zL_z^2} \quad (1)$$

where μ_{xy} and μ_z are reduced effective masses of electron-hole pairs in parallel (xy) and perpendicular (z) directions with respect to the two-dimensional crystallites. L_{xy} and L_z are the corresponding crystallite dimensions. The first term in eq 1 can be neglected because L_z is much smaller than L_{xy} . ($L_{xy} \geq 10$ nm, $L_z = 0.75$ nm, $\mu_z = 1.63m_e$ ^[3], h =Planck constant)

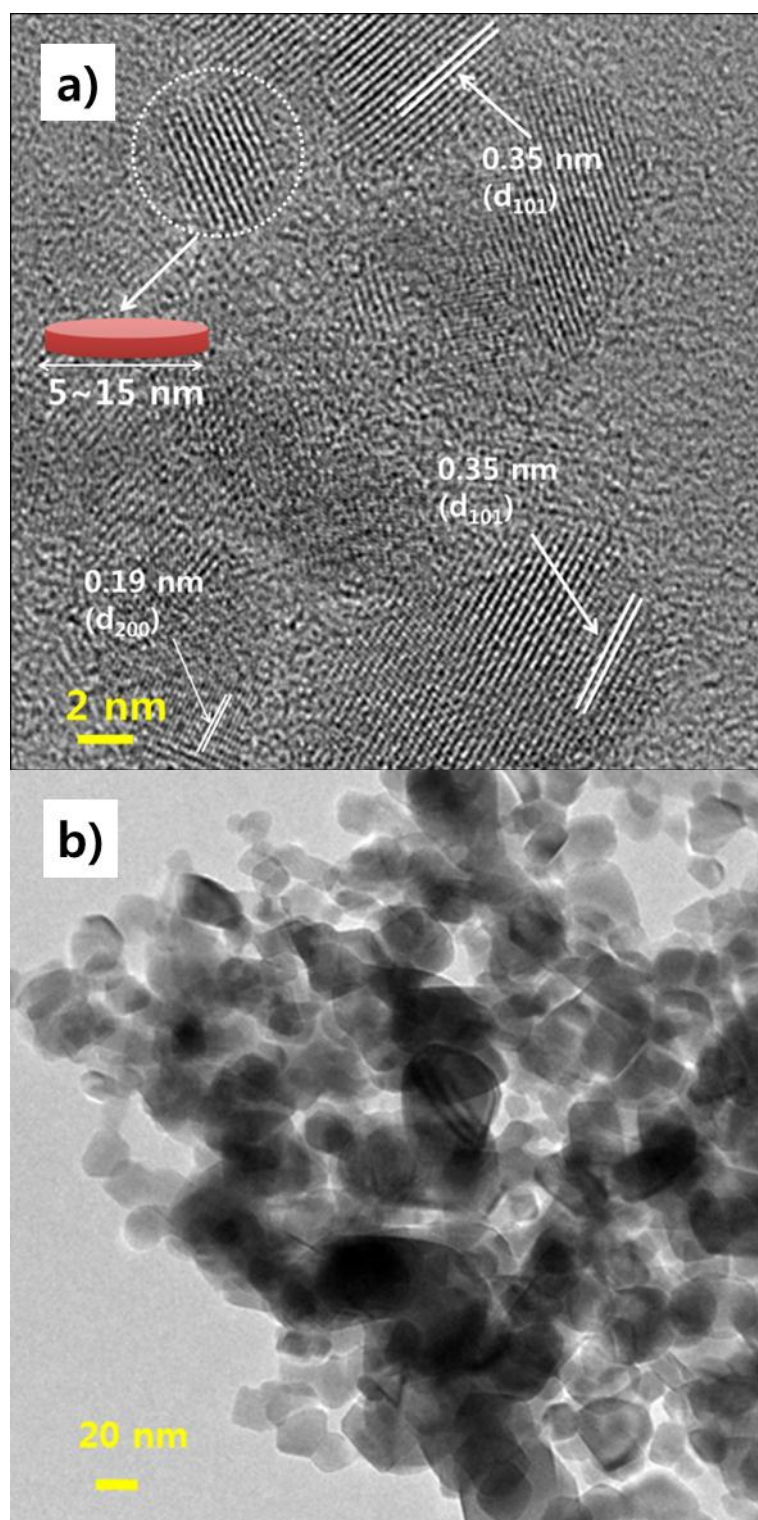


Fig. S1. HR-TEM image of (a) 2-D TiO₂-ice and (b) Degussa P25

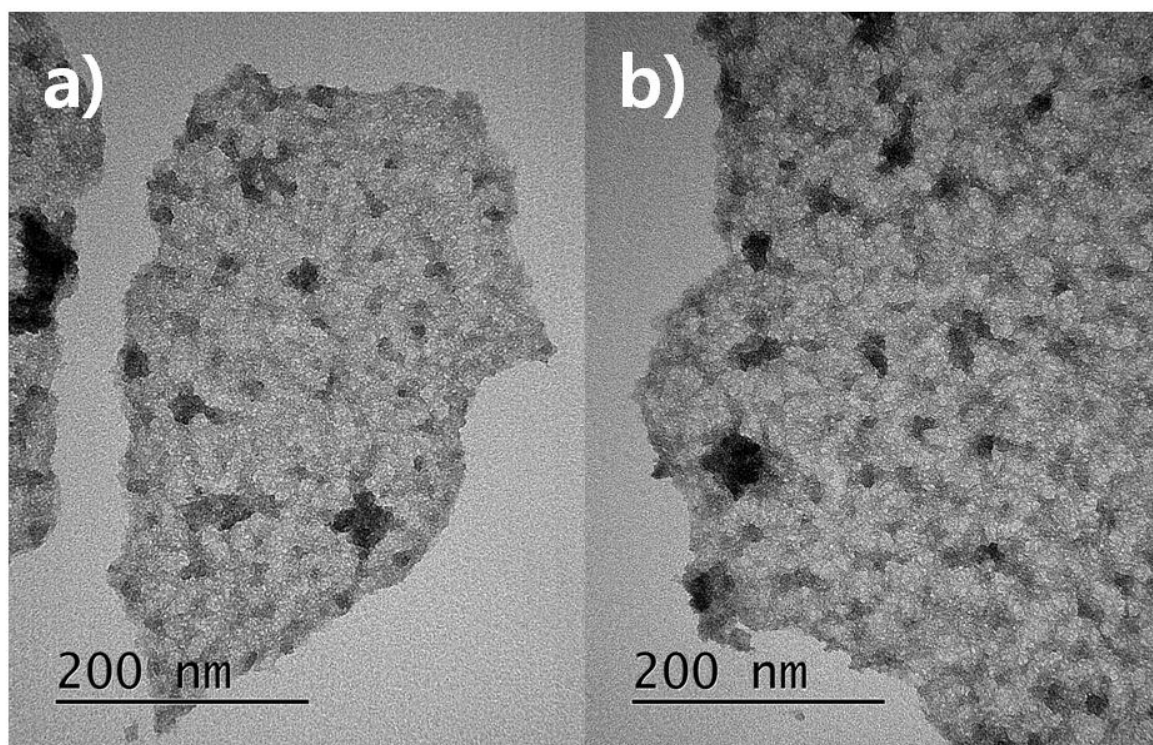


Fig. S2. Nomal TEM images of 2-D TiO₂-ice

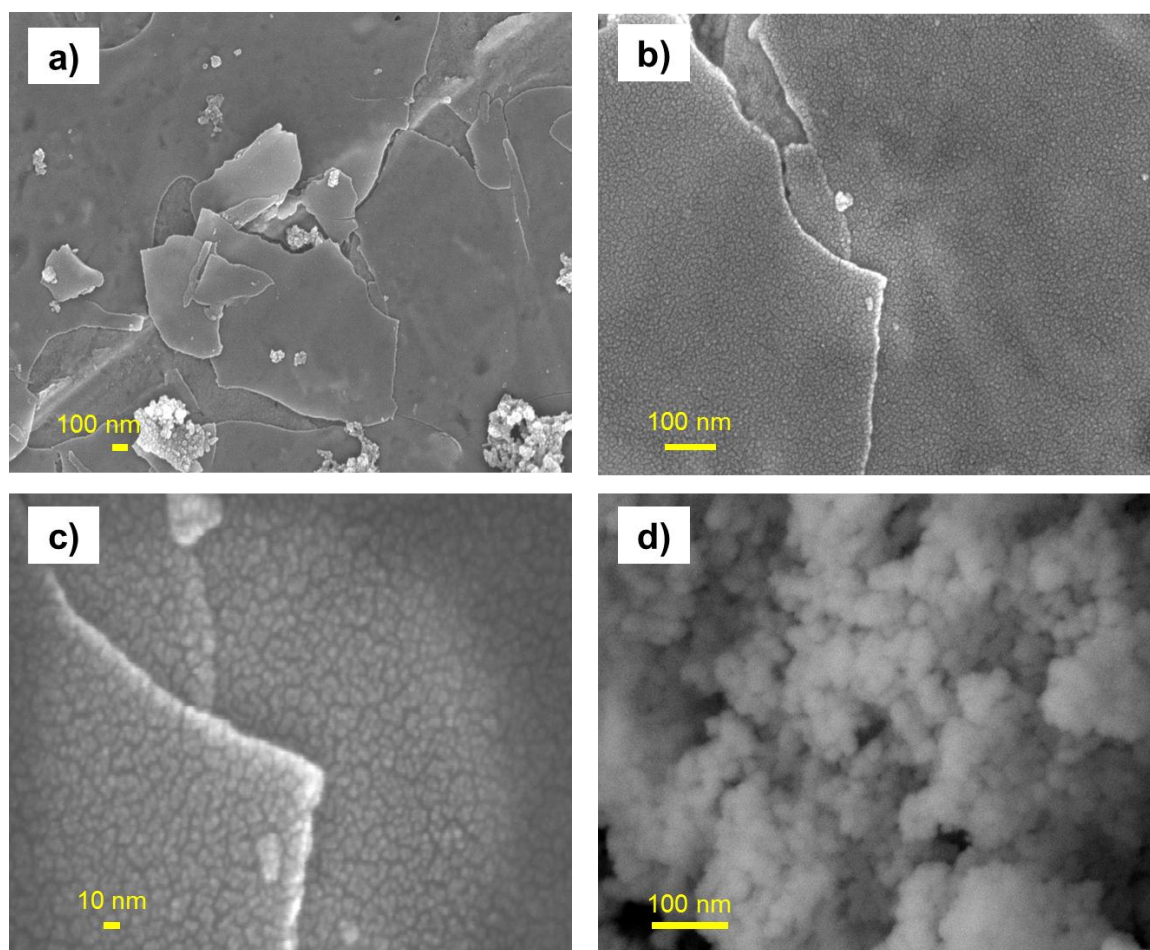


Fig. S3. FE-SEM image of (a), (b), (c) 2-D TiO₂-ice and (d) Degussa P25.

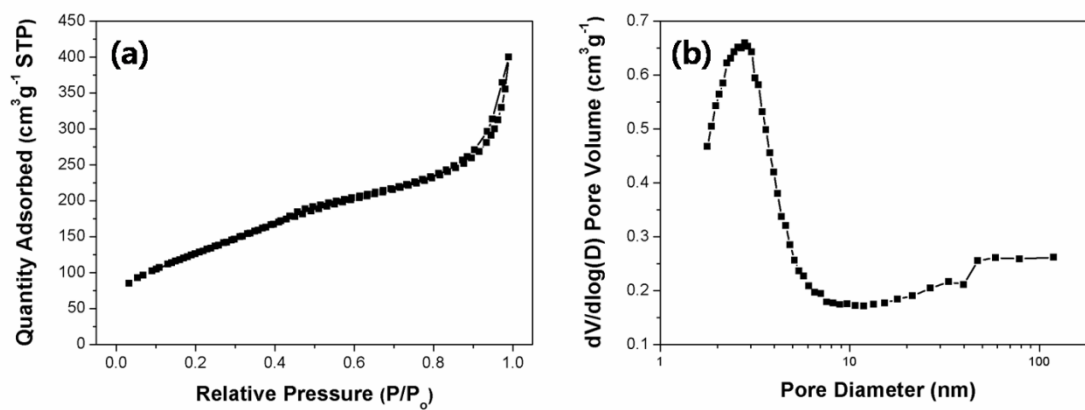


Fig. S4. (a) N₂ physisorption isotherm plot and (b) pore size distribution of 2-D TiO₂-ice.

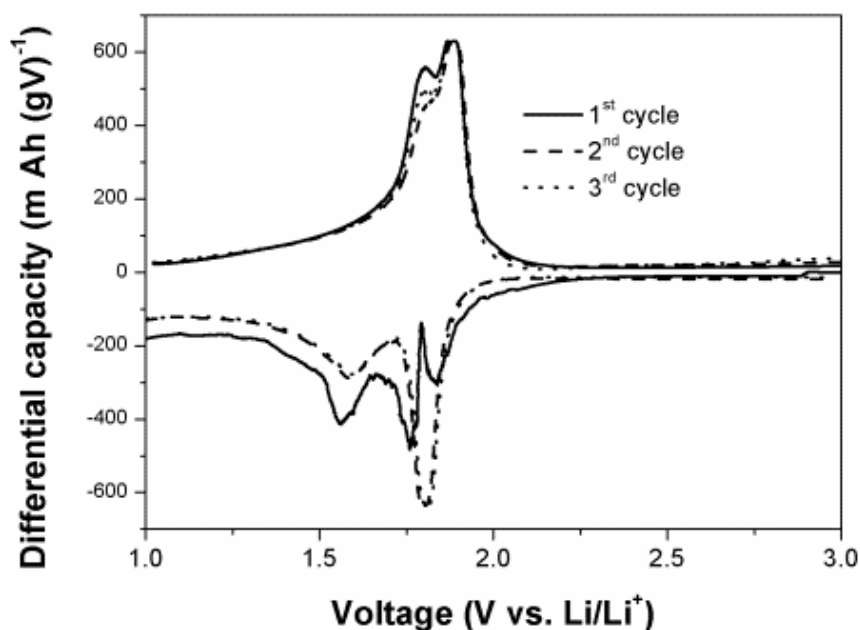


Fig. S5. Differential capacity plot of 2-D TiO₂-ice electrode in the potential range of 3.0 to 1.0 V (vs. Li/Li⁺) at current density of 34 mA g⁻¹.

This differential capacity curve of 2-D TiO₂-ice electrode is consistent with the charge/discharge curve in Figure 4 a. In the first cathodic scan, the 2-D TiO₂-ice electrode exhibited two peaks (1.85 and 1.75 V), indicating Li⁺ insertion into the different size anatase TiO₂ crystallites. From second cycle, these peaks were combined in a sharp peak centered at 1.8 V. The first anodic curve also showed two peaks at 1.79 and 1.88 V. However, the anodic 1.79 V peak disappeared during initial 3 cycles, which results in the initial capacity loss. On the other hand, unchanged anodic peak at 1.88 V signifies that the delithiation process is reversible in 2-D TiO₂-ice electrode. These cathodic/anodic peaks support that the anatase TiO₂ crystallites were well developed inside the nanodisk structure despite of its low synthetic temperature (maximum temperature is 80 °C during trying process).

At 1.6 ~ 1.0 V region, there is a broad cathodic peak centered at 1.55 V and this process is reversible. This peak is attributed to the unique characteristics of 2-D TiO₂-ice, such as high surface area and the amorphous region between crystallites. The surface capacitive behavior is possible in high surface area TiO₂ nanodisk, similar to other nano-material studies.^[4] Besides, the amorphous phase in nanodisk structure also reversibly uptakes and releases Li⁺ at lower voltage region (< 1.7 V), as confirmed by our previous study.

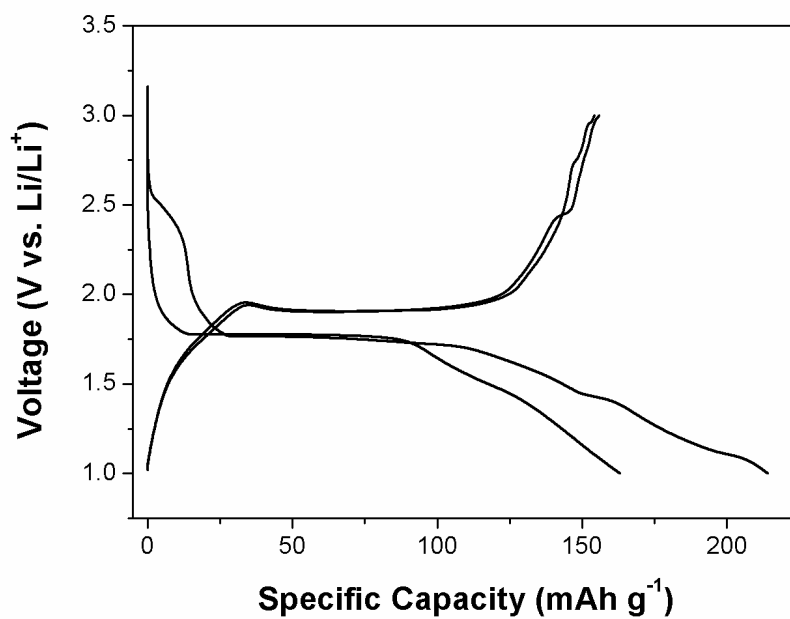


Fig. S6. Galvanostatic charge/discharge curves of Degussa P25 electrode in the potential range of 3.0 to 1.0 V (vs. Li/Li⁺).

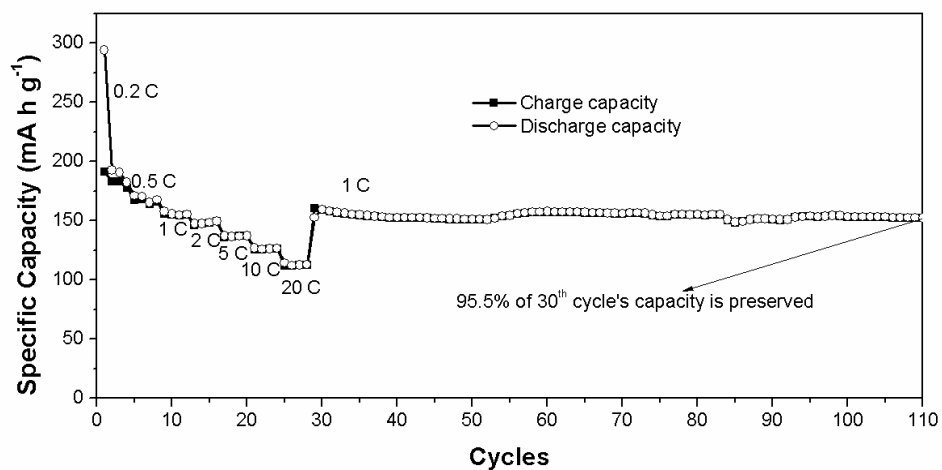


Fig. S7. Cycle performance plot of 2-D TiO₂-ice electrode at various current densities.

Table S1. Fitted impedance parameters of Nyquist spectroscopy using Randle circuit model and Zview software.

	R_s (Ω)	R_{ct} (Ω)	Z_w (Ω^{-1})
2-D TiO ₂ -ice	1.9	103	0.054
Degussa P25	4.1	204	0.036

Table S2. Electrode capacities for different TiO₂ anode materials at different measurement conditions.

Type of TiO ₂	Capacity ^a (mA h g ⁻¹)	Rate	Capacity ^b (mA h g ⁻¹)	Rate	Reference
2-D TiO ₂ -ice	191.4	0.2 C	112	20 C	This work
Freeze-dried product of the titania nanosheets	165	10 mA g ⁻¹			<i>J. Phys. Chem. Solids</i> , 2008, 69, 1447-1449
TiO ₂ nanosheets (wire shape)	185.3	2 C	85*	20 C	<i>J. Mater. Chem.</i> , 2012, 22, 21513-21518
TiO ₂ nanosheets (rectangular shape)	147.1	4 C	111.8	20 C	<i>Electrochem. Commun.</i> , 2009, 11, 2332-2335
Hierarchical spheres based on the TiO ₂ nanosheets	174	1 C	95	20 C	<i>J. Am. Chem. Soc.</i> , 2010, 132, 6124-6130
Sandwich-like, stacked ultrathin TiO ₂	191*	2 C	109*	50 C	<i>Adv. Mater.</i> , 2011, 23, 998-1002
Carbon-supported ultrathin TiO ₂ nanosheets	172.6	1 C	5 C	147.8	<i>J. Mater. Chem.</i> , 2011, 21, 5687-5692

All values are delithiation capacities. ^acapacity value at low current density condition. ^bcapacity value at high current density condition. *lithiation capacity.

Reference.

- [1]. N. Lakshminarasimhan, W. Kim, W. Choi, *J. Phys. Chem. C*, **2008**, 112, 20451
- [2]. (a) N. Sakai, Y. Ebina, K. Takada, T. Sasaki, *J. Am. Chem. Soc.*, **2004**, 126, 5851, (b) L. Kavan, T. Stoto, M. Grtzel, D. Fitzmaurice, V. Shklover, *J. Phys. Chem.*, **1993**, 97, 9493, (c) C. J. Sandroff, S. P. Kelty, D. M. Hwang, *J. Chem. Phys.*, **1986**, 85, 5337
- [3]. C. Kormann, D. W. Bahnemann, M. R. Hoffmann, *J. Phys. Chem.*, **1988**, 82, 5196
- [4] (a) B. He, B. Dong, H. -L. Li, *Electrochem. Commun.*, **2007**, 9, 425-430, (b) H. -W. Shin, D. K. Lee, I. -S. Cho, K. S. Hong, D. -W. Kim, *Nanotechnology*, **2010**, 21, 255706-255714
- [5] Y. Zhou, J. Lee, C. W. Lee, M. Wu, S. Yoon, *Chemsuschem*, **2012**, 5, 2376-2382